



## Interaction processes at the concrete-bentonite interface after 13 years of FEBEX-Plug operation. Part I: Concrete alteration

María Cruz Alonso <sup>a,\*</sup>, José Luis García Calvo <sup>a</sup>, Jaime Cuevas <sup>b</sup>, María Jesús Turrero <sup>c</sup>, Raúl Fernández <sup>b</sup>, Elena Torres <sup>c</sup>, Ana I. Ruiz <sup>b</sup>

<sup>a</sup> Institute for Construction Sciences Eduardo Torroja, IETcc-CSIC, Serrano Galvache, 4, 28033 Madrid, Spain

<sup>b</sup> Department of Geology and Geochemistry, Faculty of Science, Autonomous University of Madrid, Cantoblanco, 28049, Madrid, Spain

<sup>c</sup> Department of Environment, Research Centre for Energy, Environment and Technology, CIEMAT, Avda. Complutense 40, 28040 Madrid, Spain

### ARTICLE INFO

#### Article history:

Received 3 August 2016

Received in revised form

6 March 2017

Accepted 8 March 2017

Available online xxx

#### Keywords:

Nuclear waste storage

Underground research laboratory

Concrete-bentonite interaction

Concrete alteration

Long-term performance

### ABSTRACT

This paper evaluates the modifications created in the concrete of the FEBEX shotcreted concrete plug after 13 years in the Grimsel Test Site conditions. During this time the concrete interacted with granite groundwater and also with bentonite porewater at the concrete/bentonite contact. Three long cores and 6 small cores from different parts of the concrete plug were evaluated. Mechanical performance was not modified during this time but hydraulic conductivity increased. The main transport mechanisms involved in the alteration of the concrete were groundwater flow from the host rock to the concrete and diffusion at the concrete/bentonite interface. Leaching occurred in the concrete parts near the host rock due to the action of granite water with further portlandite dissolution. The joint action of granite groundwater and bentonite porewater has caused many changes to the concrete matrix which was located at a depth lower than 5 cm from the bentonite-concrete interface. In the first centimetre C-S-H was significantly altered, incorporating elements like Al, S and Mg which change the initial microstructure by loss of compactness. The ettringite content was very high along the length of the concrete plug due to the shotcreting technique which made use of accelerator additives that caused the formation of ettringite. An increase in the ettringite content is also shown near the bentonite barrier. Therefore, sulphate diffused from the bentonite into the concrete, causing the massive formation of new ettringite. Chloride also diffused from the bentonite barrier deeper into the concrete by up to 4–5 cm from where the formation of Friedel's salt was detected.

© 2017 Elsevier Ltd. All rights reserved.

### 1. Introduction

Deep geological disposal is considered to be the best solution for safe long-term storage of high-level radioactive waste (HLW). The waste is isolated from the biosphere by a system of multiple barriers, both engineered and natural. In this sense, great concern exists about the interaction of different components of the engineered barrier system (EBS) for HLW concept. Concrete and bentonite are two main components of the EBS in many deep geological repository (DGR) concepts (although they are absent in

DGR concepts in saline rock formation and in tuff). Both components interact during the whole service life of a storage facility. A lot of work has been dedicated to the action of alkaline concrete waters flowing towards the bentonite (Sánchez et al., 2006; Gaucher and Blanc, 2006; Fernández et al., 2009; Dauzères et al., 2010). However, less attention has been paid to the action of bentonite porewater flowing towards the concrete interface.

Underground research laboratories (URLs) are essential for providing scientific and technical information for the design and construction of disposal facilities and, most importantly, for safety assessment. Current URL focus on various long-term experiments under simulated repository conditions, full-scale demonstration tests, experiments on the disposal system, prototype repository tests and confidence building tests (Wang, 2014). The main difference between these facilities is the type of host rock (clay, salt or crystalline rocks) thus conditioning the whole EBS. The FEBEX (Full-Scale Engineered Barrier Experiment), located in the granite

\* Corresponding author.

E-mail addresses: [mcalonso@ietcc.csic.es](mailto:mcalonso@ietcc.csic.es) (M.C. Alonso), [jolgac@ietcc.csic.es](mailto:jolgac@ietcc.csic.es) (J.L. García Calvo), [jaime.cuevas@uam.es](mailto:jaime.cuevas@uam.es) (J. Cuevas), [mj.turrero@ciemat.es](mailto:mj.turrero@ciemat.es) (M.J. Turrero), [raul.fernandez@uam.es](mailto:raul.fernandez@uam.es) (R. Fernández), [elena.torres@ciemat.es](mailto:elena.torres@ciemat.es) (E. Torres), [ana.ruiz@uam.es](mailto:ana.ruiz@uam.es) (A.I. Ruiz).

environment of the Grimsel Test Site (GTS), offers a unique opportunity to perform a geochemical study of the interaction of either high pH concrete (OPC)-FEBEX-bentonite and/or granite groundwater. The FEBEX experiment background is described in section 1.1.

Concrete in direct contact with groundwater is subject to alteration processes. When cement paste comes into contact with an aqueous solution, two phenomena take place simultaneously: the transport of mass by diffusion and the chemical reactions of dissolution and precipitation (Adenot and Buil, 1992; Lovera et al., 1997; Faucon et al., 1998). The degradation of cement paste in contact with water depends not only on physical factors of concrete (such as porosity), but also on the paste chemical composition. Nevertheless, the composition of the groundwater has a strong impact on concrete degradation. The pore solution of a typical Portland cement (PC) paste is highly alkaline, so that the leaching process in deionized water starts by removing alkalis ( $\text{Na}^+$  and  $\text{K}^+$ ), followed by the dissolution of portlandite and subsequently by the leaching of calcium from silicates, e.g., C–S–H (Adenot and Buil, 1992; Faucon et al., 1998; Soler and Mäder, 2007). Aluminate phases are also affected and the dissolution/precipitation processes of AFm, ettringite and calcite have been observed (Faucon et al., 1997, 1998). A decrease in the C/S ratio of C–S–H and the incorporation of aluminum into its structure have been also described (Lovera et al., 1997). In fact, there is a continuous decrease in the calcium content of the C–S–H gel from the non-altered zone to the altered zone in contact with the groundwater inlet. However, leaching may be a slow process; 5–10 mm of leached depth have been found in concretes made of PC which have been submerged for 100 years in natural water. Progressive hydration of anhydrous cement grains have occurred during leaching, which have led to a densification of the material and new portlandite has formed from in-situ hydration (Lagerblad, 1999).

As the leaching process of Portland cement based concretes depends significantly on the composition of the groundwater, four types of reaction mechanisms have been described in the relevant literature as functions of ionic water composition:

- 1 Leaching due to the pH gradient (groundwater pH is lower than pore solution pH of concrete) leads to the dissolution of hydrated products, mainly portlandite. Degradation involves the dissolution of calcium and hydroxide ions outside the matrix, which causes an increase in porosity and transporting properties of the surface concrete (Carde and François, 1999; Mainguy et al., 2000). Leaching is accelerated by neutral and acid solutions/groundwaters (Adenot and Buil, 1992; Kamali et al., 2003), and it may be coupled with the ingress of aggressive ions such as chloride, sulphate and magnesium (Moranville et al., 2004). Thus, during the interaction and equilibration with surrounding groundwater, the changes created in the chemistry of the pore solution may result in the disintegration of the cement paste (Kari and Puttonen, 2014).
- 2 Sulphate attack on concrete: this phenomenon has been described in connection with clayey porewater solutions with high sulphate concentrations. Scenarios involving sulphate attack are shown to have the potential to seriously alter an engineered concrete barrier based on pure Portland cement. The mechanism of degradation of concrete exposed to external sulphate attack depends on exposure conditions, such as temperature, associated cation and sulphate concentration (Lipus and Punkte, 2003; Neville, 2004; Dehwah, 2007). The most well-known mechanism involves  $\text{C}_3\text{A}$  and portlandite in the cement matrix and sulphate ions (Irassar et al., 2003; Tixier and Mobasher, 2003; Maltais et al., 2004). The first stage of this mechanism is based on a diffusion-reaction based phenomenon.

Sulphate ions react with portlandite to form gypsum, which can, in turn, react with the hydration products of  $\text{C}_3\text{A}$  to form ettringite. The formation of gypsum and ettringite can be expansive.

- 3 Carbonation due to calcium leaching: this aspect is mainly relevant when the concentration of carbonates in the groundwater is high. The carbonation layer formed can act as a protective layer, as it makes the cement paste matrix denser, thus increasing its resistance against groundwater penetration (Jenni et al., 2014).
- 4 Magnesium attack: this degradation process has had limited effects in different studies which have been carried out (Santhanam, 2013), since the effect of Mg dissolved in groundwater is relatively weak in the case of low-ionic strength solutions (such as the groundwater of the GTS). Nevertheless, the effect of dissolved Mg is important in the case of aqueous solutions with elevated Mg concentrations. Moreover, in leaching tests carried out on low-pH concretes to be used in HLW repositories (Yamamoto et al., 2007; García Calvo et al., 2010), an altered front has been detected from the concrete surface in contact with the water inlet. In this altered front the decalcification of the C–S–H gels followed by the incorporation of magnesium ions from groundwater flowing into them (even forming M–S–H phases) and into the anhydrous phases (such as "magnesia nodules") has been seen. Recent results have demonstrated that Mg-perturbation has been systematically seen for low-pH cementitious materials placed in clayey, or granite environments, or in any kind of environment containing at least 3 mmol/l of magnesium in its pore solution (Jenni et al., 2014; Dauzères et al., 2016). The mineralogical phase associated with such Mg-perturbation has been identified as a Mg–Si gel-like phase.

Therefore, both the groundwater and concrete characteristics are expected to influence the concrete alteration in an underground HLW repository. In this sense, there is great concern with regard to the behavior of concrete under the long-term action of site water in representative conditions of the real storage scenario. In realistic conditions of HLW repositories, concrete durability is mainly based on its interaction with clays and/or granite groundwater. But in most of the HLW repository concepts concrete also interacts with waters from the bentonite barrier and, as mentioned above, limited attention has been paid to the action of bentonite waters flowing towards the concrete interface. From this perspective, this paper analyzes the disturbances of the concrete/bentonite EBS as a consequence of the long-term operation (13 years) of a shotcreted concrete plug in the GTS in contact with saturated bentonite (FEBEX experiment). The alteration processes detected in the concrete plug are related to both its interaction with the bentonite porewater and its interaction with the surrounding granite groundwater.

### 1.1. FEBEX experiment

The Grimsel Test Site located in the Swiss Alps was established in 1984 as a facility for underground research projects related to deep geological repositories (DGR) for radioactive waste in granite. Within this framework, the FEBEX test at the GTS was an *in situ* full-scale engineered barrier experiment performed under natural conditions and designed to assess the Spanish DGR reference concept in crystalline rock (Huertas et al., 2006): canisters are placed horizontally in drifts surrounded by a clay barrier constructed from highly compacted bentonite blocks (see Fig. 1A).

A gallery of 70 m in length and 2.28 m in diameter was excavated in the granite host rock, crossed by a lamprophyre dyke in which two electrical heaters were placed (4.5 m long and 0.9 m

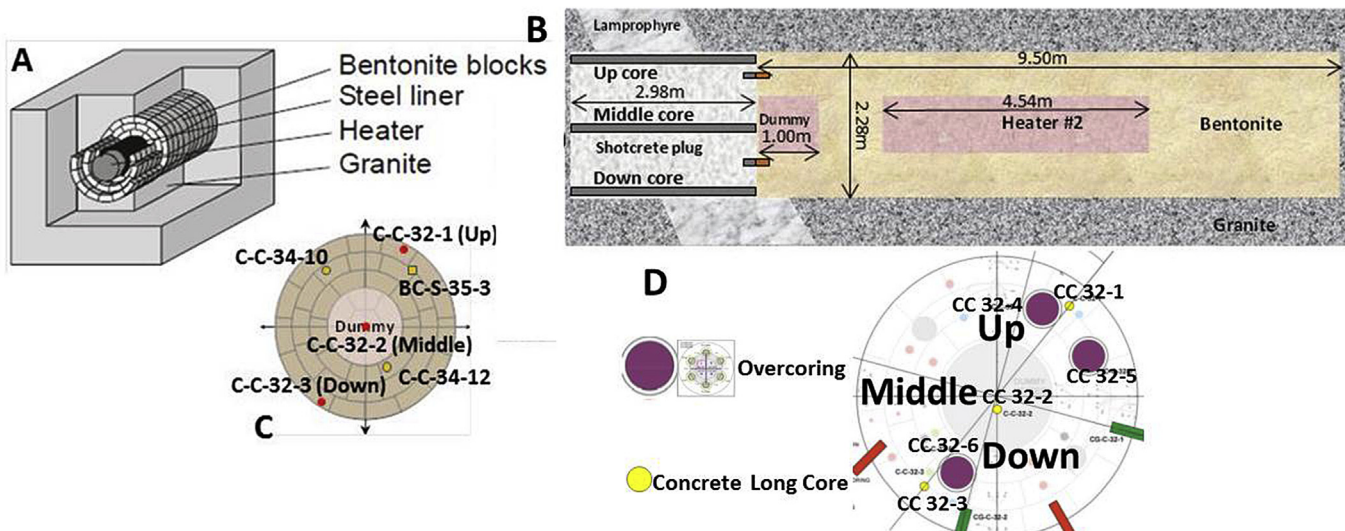


**Fig. 1.** A: Scheme of the engineered barrier experiment installation (FEBEX). B: lateral view of the FEBEX installation and location of the concrete cores evaluated in this paper and in the Part II of the study (Fernández et al., 2017). C: frontal view of the FEBEX installation and location of the concrete cores evaluated in this paper and in the Part II of the study. D: location of the overcores.

in diameter), separated from each other by 1 m and surrounded by a 0.7 m thick FEBEX bentonite barrier (density of 1.7 g/cm<sup>3</sup>, water content of around 14%). Various sensors were installed to monitor each material. A concrete plug (2.7 m thick) sealed the test. The test was initiated in February 1997. The heaters simulating the thermal effect of the waste were set to a temperature of 100 °C, while the bentonite buffer was slowly hydrating in a natural way with groundwater infiltrating from the granite. After five years (February 2002) of uninterrupted heating, the heater which was closer to the gallery entrance was switched off. In the following months the heater and all the bentonite and instruments preceding and surrounding it were retrieved. The gap left by the heater was filled with a metal cylinder (dummy) and the remaining part of the experiment was sealed again with a sprayed concrete plug. The plug was constructed in two parts: a first section (the one closer to the bentonite) with a thickness of one metre and a second one of two metres. Both concrete plug sections were constructed using the shotcreting technique. An impermeable polymer layer (3–4 cm) was sprayed between both sections. New sensors were installed in the buffer, and a second operational phase started in 2002 with the configuration shown in Fig. 1B. The experiment was permanently dismantled in 2015 (more details can be found in ENRESA (2006) and <http://www.grimsel.com/gts-phase-vi/FEBEX-dp/FEBEX-dp-introduction>). It is remarkable that based on the temperatures recorded by sensors in different sections of the experiment before the shut-down of the heater, the temperature of the concrete was below 28 °C (Martínez et al., 2016). Thus, the modifications created in the concrete were related to its interaction with the granite groundwater and/or the bentonite porewater, but not to the existence of elevated temperatures.

In the FEBEX experiment the local geochemistry is driven by granite groundwater chemistry, concrete chemistry (high pH, mineralogy, ageing), and bentonite chemistry (exchangeable cations, smectite crystal-chemistry, secondary mineral dissolution-precipitation reactions, and porewater chemistry). Table 1 summarizes the chemical composition of the granite groundwater at the GTS and the bentonite porewater. The granite groundwater at the GTS has a very low salinity (total dissolved solids < 10 mg/l) and it is composed of Na-Ca-HCO<sub>3</sub> (pH ≈ 9) (Buil et al., 2010). This porewater was expected to saturate concrete and bentonite

through contact with the surface galleries. Major chemical gradients in the EBS system were related to concrete interfaces and bentonite interfaces. In fact, FEBEX bentonite porewater saline (~0.3 M NaCl; pH = 7.4, type Na-Mg-Ca-Cl-SO<sub>4</sub>-HCO<sub>3</sub>) (Fernández et al., 2004; Fernández and Villar, 2010) compared to the GTS groundwater.

Two investigations support the task of assessing concrete durability in a DGR through the post-mortem characterization of the aged shotcreted plug from the second operational phase of the FEBEX test. This contribution (part I) is related to the interaction of the concrete plug with the bentonite porewater and with the surrounding granite groundwater. Another contribution (part II) to this issue deals with the analysis of the physical, chemical and mineralogical changes that occurred in the clay and in the concrete through their interaction and with the extension of the alteration front in both materials (Fernández et al., 2017).

## 2. Experimental procedure

### 2.1. Materials

As part of the dismantling operations in the FEBEX test, three long cores with outer diameters of 78 mm were drilled by mid-February 2015, sampling the shotcrete plug (around 3 m) as shown in Fig. 1B, for the characterization of the aging of concrete and interaction with bentonite porewater and granite groundwater. The samples were identified as C-C-32-1, C-C-32-2 and C-C-32-3 following the codes of the sampling plan for the FEBEX dismantling operations (Bárcena and García-Síñeriz, 2015). The first 2.7–2.8 m of the cores were drilled under wet conditions whereas the last 10–20 cm were drilled under dry conditions. After drilling, the cores were packed, first wrapped in a humid cloth, and later put inside a plastic bag under vacuum to prevent drying and carbonation from the atmosphere. Fig. 1C presents a front view with the location of the three long cores:

- Sample C-C-32-1 was positioned on the upper right side of the central gallery axis, near the granite (≈ 15 cm). It will be referred to as the Up core in this paper.

**Table 1**

Chemical composition of the granite groundwater and the bentonite porewater (Buil et al., 2010\*; Fernández et al., 2004; Fernández and Villar, 2010; Garralón et al., 2016\*\*).

Water	pH	mg/l								
		Na	K	Ca	Mg	Cl	SO <sub>4</sub>	HCO <sub>3</sub>	F	SiO <sub>2</sub>
*Granite groundwater	9.0	8.71	0.31	7.33	0.02	0.48	7.49	24.1	4.23	9.68
**Bentonite porewater	7.4	2100	15	510	390	4000	1260	133	—	—

- Sample C-C-32-2 was located 10 cm down the central gallery axis and represents the concrete farthest from the interaction with granite groundwater. Since this core was not in contact with the bentonite it is expected to be less altered than the other two long cores. It will be referred to as the Middle core in this paper.
- Sample C-C-32-3 was drilled onto the lower left side of the central gallery axis, near the granite ( $\approx 15$  cm). A constant backflow of water was observed during dry drilling since they looked wet during their retrieval. This backflow of water did not continue after 24 h of the completion of the drilling. (García-Sineriz et al., 2016). It will be referred to as the Down core in this paper.

In addition, as shown on Fig. 1D, three overcorings were made named as CC 32-4 and CC 32-5, near the Up core, and CC-32-6, near the Down core. During the sampling of overcoring, short concrete cores of 4 cm diameter and 10 cm long were obtained. Two of these short concrete cores which formed each overcoring were also used in this study to complete the results obtained with the long cores. In fact, these small cores were used to complete the evaluation of the pore fluid composition (described in section 2.2).

In this paper, only the concrete of the first section of the plug is discussed since it is the section in direct contact with the bentonite barrier. The concrete composition of this first section of the plug is shown in Table 2. The initial compressive strength of the concrete was 32 MPa and the initial hydraulic conductivity of the concrete was  $4.3 \cdot 10^{-11}$  m/s. To identify the interaction of porewater from saturated bentonite with concrete most of this study was carried out on samples of concrete up to a depth of 10 cm from the bentonite contact, although some tests were made at distances farther from the bentonite (where the influence of bentonite porewater was expected to be very low or even ineffective). The evaluation of the concrete at further distances from the bentonite ( $>10$  cm) allows the identification of the modifications created in the concrete only through its interaction with the granite groundwater. Thus, this evaluation of the concrete alteration at different distance from bentonite and from host rock was helpful in demonstrably separating the effect of the groundwater and the effect of the bentonite porewater on the concrete.

As shown in Fig. 1, another two short cores C-C-34-10 and 12 were also extracted from the plug. These cores were dry-drilled

with a diamond coring machine with the aim of sampling the shotcrete/bentonite interface to study the shotcrete/bentonite interface in the upper and lower half of the plug, respectively. Moreover, the concrete/bentonite interface was addressed in greater detail in a sample carefully collected by hand, which was located in the right "Up" zone and identified as BC-S-35-3. However, the corresponding results of these three cores are discussed in part II on this issue (Fernández et al., 2017).

## 2.2. Methods

In order to evaluate the modifications in the concrete performance after 13 years of the operation of the plug, the compressive strength of the concrete cores was determined in samples of  $60 \times 120$  mm cut at  $\approx 10$  cm from the bentonite barrier (or the dummy in the Middle core) following the UNE-EN 1015-11 standard. The hydraulic conductivity was evaluated in samples of  $50 \times 50$  mm sized at 50 cm from the bentonite barrier (or the dummy in the Middle core). The samples were placed between two cylinders of methacrylate containing holes for the inlet and outlet of water. The device and the methodology used have been described elsewhere (García Calvo et al., 2010). The granite water from the Grimsel site was used, since hydraulic conductivity is influenced by the groundwater considered. Therefore the conditions in the laboratory had to be as similar as possible to those at the real site. Air pressure of 0.5 bars was applied to accelerate the passing of water through the concrete sample.

Microstructural tests were performed to characterize concrete–granite groundwater interaction and concrete–bentonite porewater interaction. Pore solution pH and water soluble ions were measured. For the water soluble components of concrete the test followed was based on mixing a portion of powdered concrete with deionized water at a solid/liquid ratio = 1 and stirring the resulting slurry for 5 min. The suspension was vacuum filtered and then the pH and the ionic composition were determined. The pore solution pH was measured as reported by Alonso et al. (2013) using a pH meter with temperature compensation and a combination pH electrode specifically designed for measuring suspensions in the pH range of 7–14 (associated error  $\approx 0.05$ ). In order to prevent the carbonation of the cementitious material samples, both the leaching tests and the pH measurements were performed under nitrogen atmosphere. Na, K, Ca, Si, Al, Mg, S contents were determined using a plasma mass spectrometer (ICP-OES- 725-ES-Varien). The detection limits (in ppm) of these elements were 0.035, 0.052, 0.017, 0.069, 0.018, 0.009 and 0.390, respectively. The total Cl content was determined after total dissolution of the solid using nitric acid (quality "per analysis" from Scharlau) followed by a potentiometric titration of Cl. The results are expressed as % by cement (or binder) mass.

The alteration of the solid phases of the matrix of the concrete was determined using several characterization techniques. XRD patterns were recorded at room temperature with the interval  $5^\circ < 2\theta < 60^\circ$ , with a step size of  $2\theta = 0.01973^\circ$  and 0.5 s per step. An X8 Advance X-ray diffractometer from Bruker with a Cu source of 2.2 kW and an ultra-fast RX Lynxeye detector with a Ni K-beta filter was used. DTA/TG data were obtained using a STD Q600 V 20.9

**Table 2**

Concrete composition of Section 1 of the shotcrete plug.

Concrete Section 1	Content
CEM II A-L 32.5R	430 kg/m <sup>3</sup>
Water	170 kg/m <sup>3</sup>
Nanosilica (Meyco MS600)	30 kg/m <sup>3</sup> (6.5% in cement weight)
Aggregate 0–8 mm	1700 kg/m <sup>3</sup>
Steel fibres (Dramix ZP 306)	50 kg/m <sup>3</sup>
Polypropylene fibres	800 g/m <sup>3</sup>
Superplasticizer Glenium T803	1.5% in cement weight
w/c	0.4
Curing Compound (Meyco TCC 735)	1% in cement weight
Accelerator (Meyco SA 160E) Al based	6% in cement weight

Build 20. The samples were heated to 1000 °C at a heating rate of 10 °C/min using nitrogen as a medium under static conditions. Alumina powder was used as a reference material. Backscattered electron microscopy (BSEM) images were obtained using a Hitachi S-4800 scanning electron microscope equipped with a BRUKER 5030 energy dispersive analyser under the following conditions: 20 kV accelerating voltages and a beam current of 20  $\mu$ A. The samples were embedded into an epoxy resin, cut, polished and then coated with carbon.

In the three long cores the characterization tests were made at different depths from bentonite contact: 0, 1, 2, 3, 4, 5, 6, 7 and 10 cm. In the short cores similar depths were considered. For comparison, some tests were also carried out on the long cores at other distances (50 and 85 cm) from the bentonite barrier (Up and Down cores) and the dummy canister (Middle core).

### 3. Results and discussion

#### 3.1. Modifications in concrete performance after 13 years of the operation of the concrete plug

The initial compressive strength of the concrete was 32 MPa. After 13 years of operation, the compressive strength of the Up core was  $30.5 \pm 3.9$  MPa, that of the Middle core was  $30.2 \pm 3.8$  MPa and that of the Down core was  $29.9 \pm 2.2$  MPa. Thus, a very slight compression strength decrease can be seen that could be a consequence of the aging of the concretes. Therefore, the modifications created in the microstructure of the concretes (see sections 3.2 and 3.3) have not yet limited its mechanical performance although the mechanical strength of the concrete cannot be measured in the parts in contact with the bentonite barrier.

Regarding the hydraulic conductivity, the values obtained were:  $4.2 \cdot 10^{-10}$  m/s for the Up core,  $3.5 \cdot 10^{-10}$  m/s for the Middle core and  $5.0 \cdot 10^{-10}$  m/s for the Down core. These values are one order of magnitude lower than the initial one ( $4.3 \cdot 10^{-11}$  m/s) so the interaction of the concrete with the surrounding groundwater had an influence on this parameter. This increase in hydraulic conductivity is related to the leaching processes detected in the concrete and described in the following sections. The higher values obtained in the Up and the Down cores are related to the greater influence of these leaching processes on these zones of the concrete plug. The increase in the hydraulic conductivity of the concrete could imply that although the principal transporting mechanism is expected to be diffusion (since the concrete was expected to be saturated), there was some water flow within the concrete that would force the acceleration of the movement of soluble ions from the saturated pores.

#### 3.2. Changes in the content of soluble ions due to the simultaneous interaction of granite and bentonite water with the concrete plug

The very low ionic strengths and the pH of around 9 of the granite groundwater of the GTS (Buil et al., 2010) favoured the dissolution of soluble components followed by a pH decrease of the concrete pore solution, as shown in Fig. 2. The pH of the Middle concrete core, measured at different distances from the dummy, is always above 12.65, although at 1 cm it is slightly lower than at further distances from the dummy canister. In fact, at 2 cm it was already above 12.8. However, the Up and Down concrete cores show lower pH values, up to 5 cm from the bentonite barrier, and the values measured in the Down core are actually slightly lower than the values of the Up core. In fact, at 1 cm from the bentonite both cores clearly show pH values below 12.2 (even 12 in the case of the Down core). This decrease of pH could be the consequence of several processes, mainly alkali (Na and K) leaching followed by

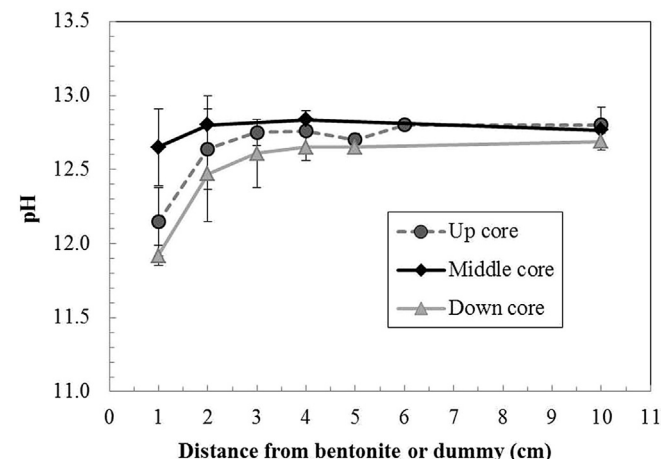
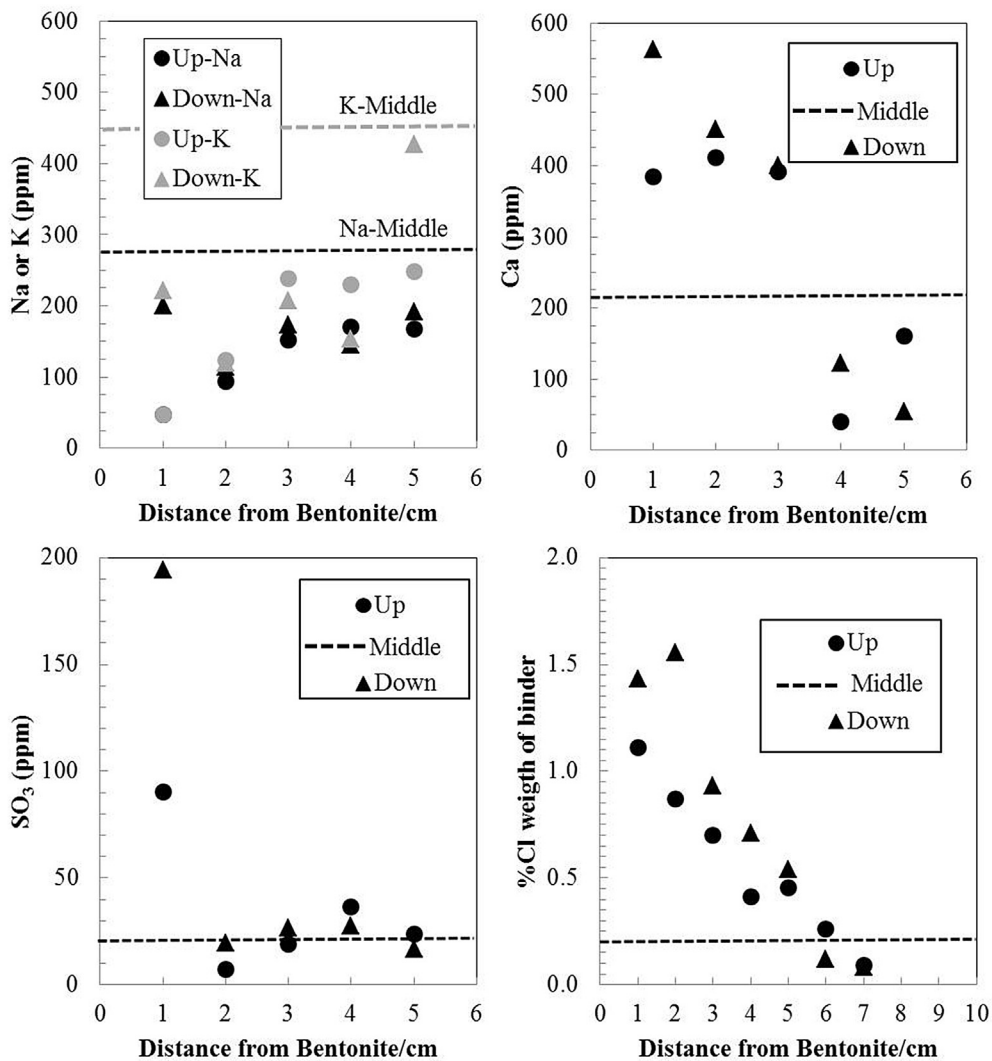


Fig. 2. Pore solution pH changes in concrete plug near bentonite interface compared with Middle concrete (no-groundwater interaction).

portlandite dissolution. Portlandite dissolution is commonly observed in OPC concretes in contact with granite water (Soler and Mäder, 2007). It is well known that below pH = 12.5 the presence of portlandite is limited or even not seen at all in the cementitious matrix.

Furthermore, the main water soluble ions of the concrete near the bentonite (Na, K, Ca,  $\text{SO}_4^{2-}$ , Cl) show differences between the Middle concrete samples and Up and Down samples (Fig. 3). In Fig. 3 the results from the Middle concrete are shown as the mean content measured between 1 and 5 cm from the dummy canister since the obtained values are quite similar for each sample. The results shown in Fig. 3 suggest the coupling of different processes depending on the source of water interacting with the concrete and its composition. First of all a decrease in the content of alkalis, both Na and K, can be seen in the Up and Down cores in comparison to those measured in concrete from the Middle core of the plug. This confirms the leaching of alkali ions due to the action of granite water which further coincides with the decrease of pH observed in Fig. 2. However, the Ca concentration is higher in the Up and Down concrete cores in comparison to that of the Middle concrete core. This increase in the soluble Ca content of the Up and Down cores can be mainly explained by the ingress of Ca from the bentonite once it is saturated with granite water and when some redistribution in the occupancy of cation exchange sites occur. Waters from the FEBEX bentonite are rich in Ca ions (Fernández and Villar, 2010; Garralón et al., 2016). Thus, Ca diffusion from the bentonite pore-water into the concrete porewater has to play an important role in explaining the results. In fact, there is evidence based on  $\delta^{13}\text{C}$  isotopic signature in bentonite carbonates indicating calcite redistribution from the bentonite to the concrete interface (Fernández et al., 2017). The interaction of bentonite porewater with the cement paste concrete is further confirmed by the analysis of dissolved sulphates and total chlorides in the Up and Down concrete samples near the bentonite. Both anions are present in the Up and Down concrete samples at depths close to bentonite while their content is very low in the Middle concrete core at similar depths (with no direct contact with bentonite or granite waters). Nevertheless, a clear difference can be seen in the penetration depth between both anions. While Cl penetrated faster, even up to 5 cm from the bentonite barrier, the high sulphate contents can only be detected in the very first cm of the concrete close to bentonite. The studies of several interfaces with bentonite reveal high sulphate concentrations close to the bentonite surface, while for chloride the distribution is more heterogeneous, in agreement with its more



**Fig. 3.** Main water soluble ions and total Cl contents in concrete plug near bentonite interface compared with results from Middle concrete.

mobile behavior (Cuevas et al., 2016). The different reaction capacity of the cement for the two anions must also influence the different penetration depths detected.

Other differences can be seen in the soluble contents of Si, Al and Mg, although their concentrations are below 5 ppm in all cases. Their presence is almost negligible in the Middle concrete core (0.07, 0.04 and 0.05 ppm, respectively). After interaction with granite and bentonite waters, an increase is detected for all elements up to levels of 7, 1 and 0.3 ppm (Si, Al and Mg respectively). Certainly, these contents are not significant in comparison with the Na, K, Ca, SO<sub>3</sub> and Cl contents, but in all cases, they are at least two orders of magnitude higher than the values measured in the Middle concrete core. Thus, these elements are supposed to diffuse from the bentonite barrier into the concrete.

### 3.3. Concrete solid phase alteration due to interaction with granite and bentonite waters

The solid phases of the cement paste from the concrete plug also show changes as a consequence of the interaction with granite groundwater of GTS and bentonite porewater. Fig. 4, left, shows the XRD data of the concrete of the Up core at different depths, while Fig. 4, right, shows the XRD from the Middle concrete core at

different depths from the dummy canister (since Middle core was not in direct contact with the bentonite barrier). The XRD data are shown as between  $2\theta$  values of 5 and 20° in order to outline the more interesting results. Fig. 5 shows the DTG/TGs of the 3 long concrete cores at 50 cm from the bentonite barrier.

Two important aspects can be seen in both figures. Portlandite can be clearly seen in the Middle concrete (Fig. 5), while the corresponding DTG peak is less prominent in Up and Down cores. In fact, the percentage of weight loss associated with portlandite in Up and Down concretes at 50 cm from bentonite is very low compared to the loss obtained in the Middle core at the same distance. This portlandite decrease at this distance from the bentonite means the dissolution of this hydrate due to granite groundwater interaction. Thus, a leaching process caused by water flow from the granite within the concrete occurred. However, regarding the XRD of the Up concrete core (Fig. 4), portlandite actually disappears at depths close to the bentonite barrier while portlandite reflections are clearly detected in the XRD of the Middle concrete core at all depths evaluated. Thus, the dissolution of portlandite is caused by the combined action of two solutions: granite groundwater and bentonite porewater.

Ettringite nodules can be seen in high numbers along all the concrete core lengths. In fact, the intensity of the ettringite

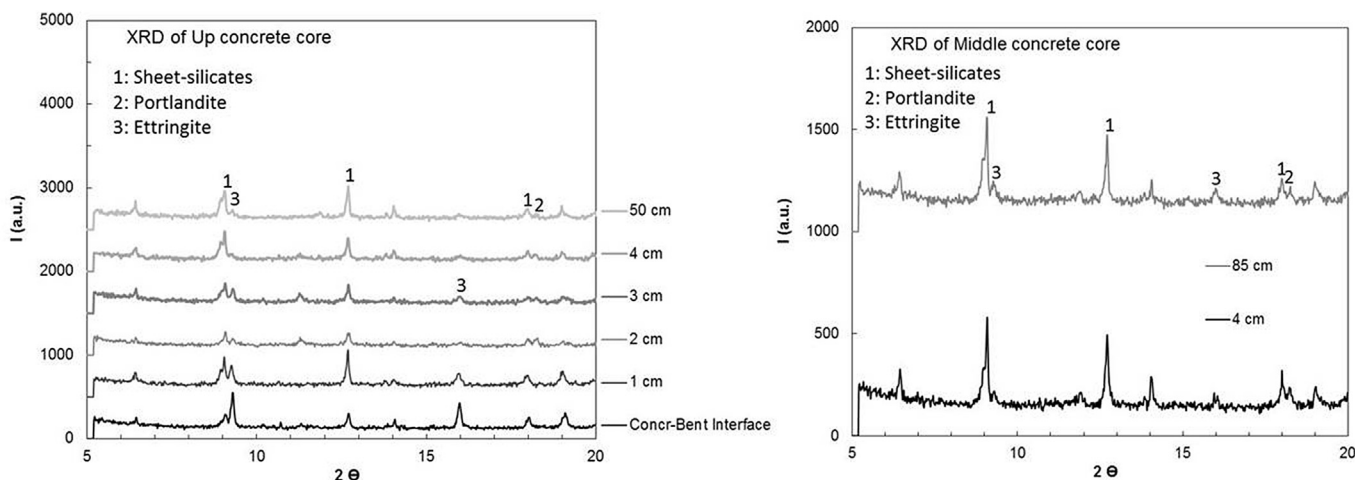


Fig. 4. Left: XRD of Up concrete core at different depths from bentonite barrier; right: XRD of Middle concrete core at different depths from dummy.

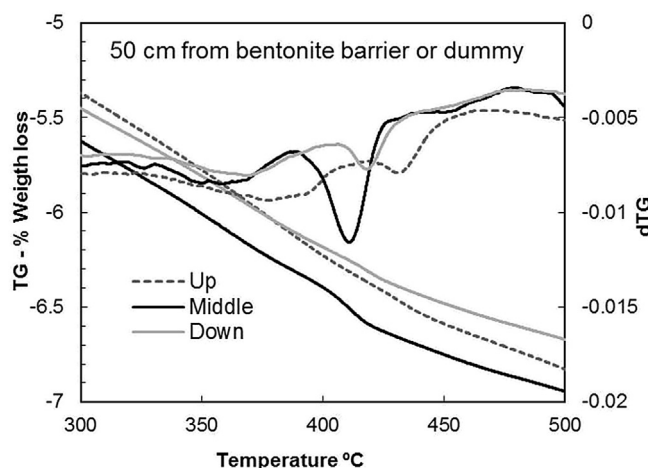


Fig. 5. Detail of dTG/TGs of all the cores at 50 cm from bentonite barrier or dummy.

reflections is as important as the intensity of the second portlandite reflection ( $2\theta = 18.09$ ). This high intensity of ettringite reflections, higher than that which is usually found in a conventional concrete based on Portland cement (even in concretes with high  $C_3A$  content), is related to the use of the shotcreting technique to construct the plug i.e. the use of accelerator admixtures. Although the cement composition is unknown it is shown in Table 2 that at least 6% of the accelerator (in cement weight) was used to shotcrete the concrete. According to the manufacturer this accelerator had a high Al content, thus promoting ettringite formation to obtain the initial fast hardening required. However, the intensity of the ettringite peaks is even more important at depths close to the bentonite barrier as Fig. 4 clearly shows. In fact, the maximum intensity of this peak can be seen at the concrete-bentonite interface. The XRD data of the Down core (not shown) are similar to the results obtained for the Up core while in XRD data from the Middle core the ettringite peaks near the dummy are less pronounced. Therefore, although the ettringite content is very high along all the concrete core lengths, there is a clear increase near the bentonite due to its interaction with the concrete. Porewater from bentonite is rich in sulphate, thus, sulphate diffusing into concrete will interact with the Al present in cement paste or this element can even be supplied locally by the bentonite minerals dissolved at the alkaline interface.

Finally, BSEM results are discussed. Fig. 6 shows the different parts of the concrete cores. A large number of ettringite crystals are detected in all cases. In the BSEM image of the Middle core, ettringite nodules of at least  $100 \mu\text{m}$  can be clearly seen and they fill the pore space in many cases. Few microcracks are detected but they are not related to ettringite since they are also found in the bulk of the cement paste. They can be attributed to shrinkage phenomena due to drying or heating during hardening and hydration. In this sense, the initial ettringite formed in the concrete plug does not seem to induce expansive phenomena. In one of the images from the Down core (Fig. 6, bottom left) a clear increase of the ettringite is detected very close to the bentonite contact. Therefore, the promotion of a massive secondary ettringite formation as a consequence of the interaction of the concrete with the bentonite porewater is shown.

This ettringite formation near the bentonite barrier is even more evident in the S mappings from the Up core (Fig. 7). The presence of many ettringite nodules on all the concrete can be seen, but a clear increase in the S content is detected near the bentonite barrier. In fact, although small ettringite nodules can be detected, a massive ettringite formation is primarily observed in this zone.

In the regions near the bentonite (2–3 cm) the presence of another type of crystal can also be seen in the Up and Down cores, but not in the Middle core (Fig. 6, up right, BSEM image from the Up core). These crystalline phases have been identified by EDS as Friedel's salt. Although their formation is not very pronounced, small platelets of Friedel's salt are detected in the cement paste, but at a farther distance from the bentonite barrier than the massive ettringite formation mentioned above. The penetration of Cl anions into the concrete is faster than that of sulphate, thus allowing the binding of Cl with the cement hydrates, leading to the subsequent formation of the Friedel's salt. As a second step, the continuous diffusion of sulphates may progressively substitute Friedel's salt with ettringite, leaving free chlorides that diffuse deeper into the concrete. This deeper penetration of the Cl ions from the bentonite barrier coincides with the results shown in Fig. 3.

Another alteration phenomenon was detected in the cement paste (Fig. 6, down-right). Different phases with different colors (dark-grey and light-grey) and crystalline appearances can be seen, that differ significantly from the cement paste of the concrete of the Middle core. A loss of density and microcracking can also be seen. EDS microanalysis of the different phases mentioned above are shown in Figs. 8 and 9. The corresponding EDS measuring points shown are indicated in the BSEM images of both figures.

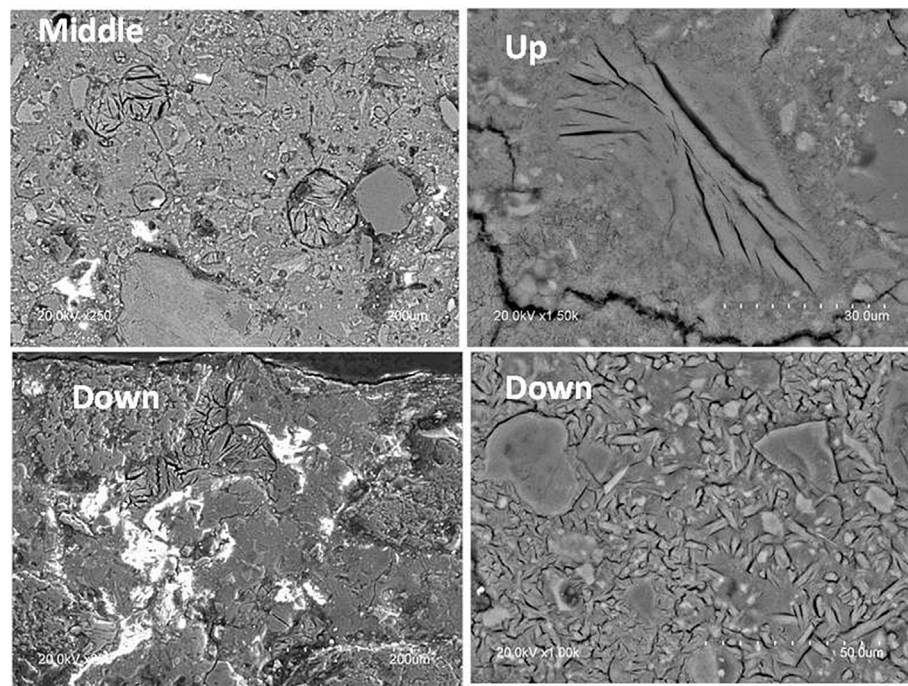


**Fig. 6.** BSEM images of Middle ( $d = 85$  cm), Up and Down concretes ( $d = 0$ –1 cm) ( $d$  = distance from bentonite barrier or dummy). Image up-left: x250; up-right: x1500; down-left: x250; down-right: x1000.

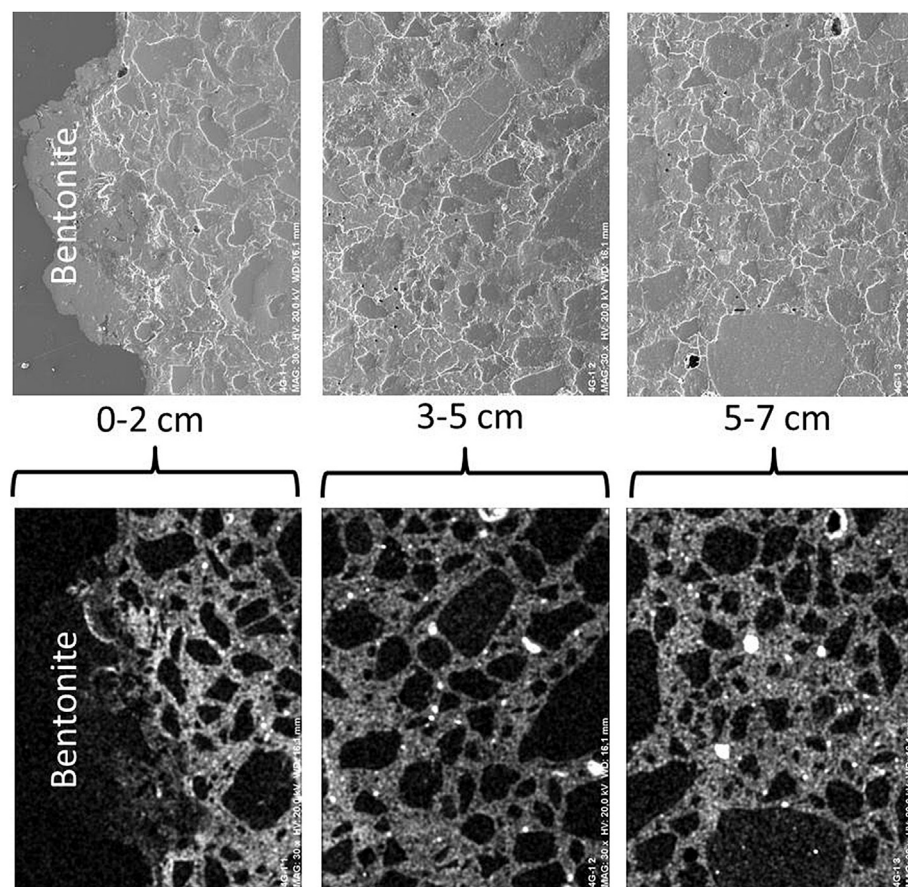


**Fig. 7.** BSEM images (x30) and S mapping of Up concrete at different depths from bentonite barrier.

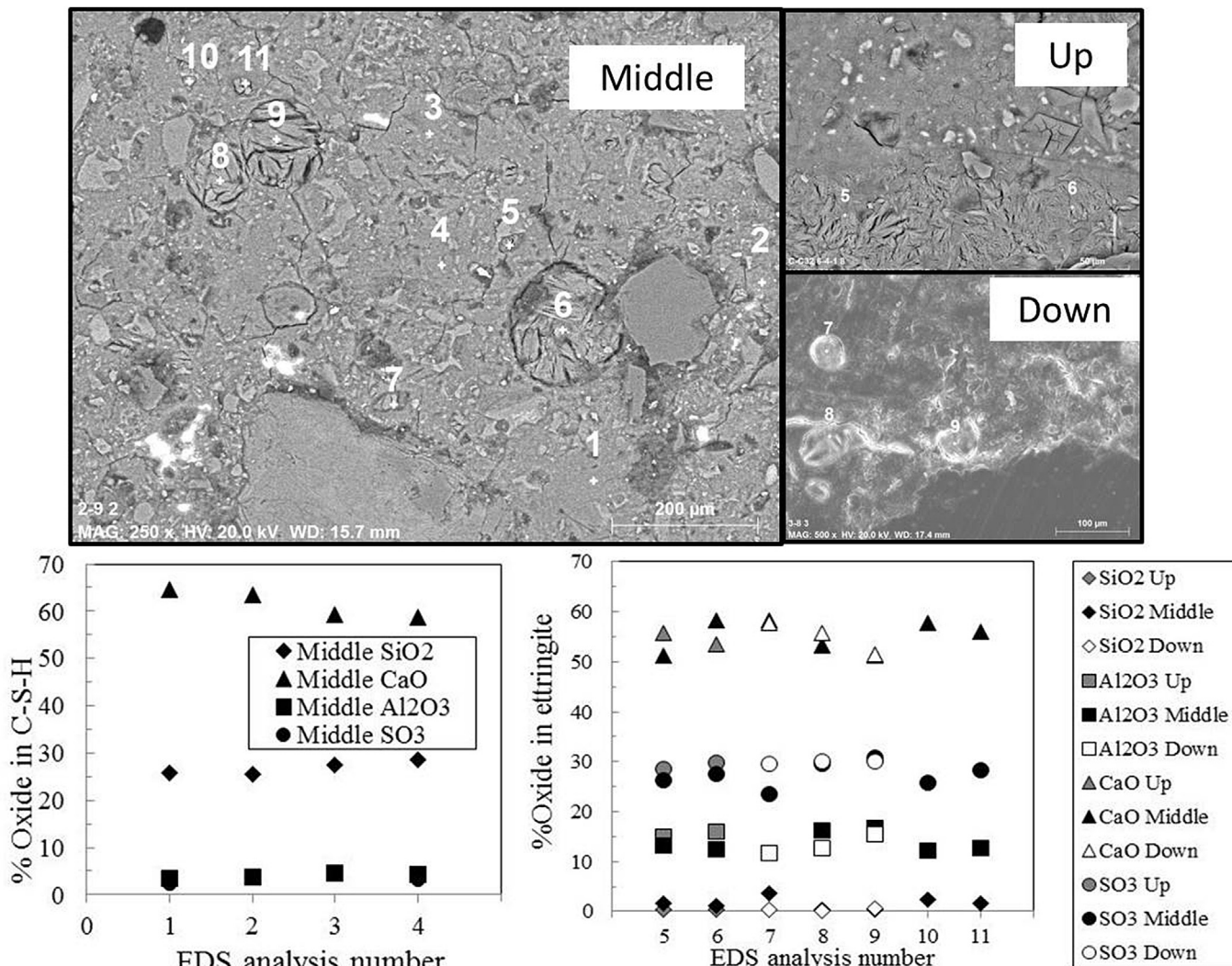


**Fig. 8.** Up-left: BSEM of Middle core (x250); up-right: BSEM images of Up core (x1000) and Down core (x500); down-left: EDS analysis of the C-S-H of Middle concrete core; down-right: EDS analysis of ettringite in Middle, Up and Down concrete near bentonite barrier or dummy.

Concerning the cement paste of the Middle core (Fig. 8 up-left), the % of the element expressed as oxide indicates that the content of SiO<sub>2</sub> is that which is commonly found in C-S-H gels of a conventional Portland cement paste, while the content of CaO is very high as a consequence of the limestone filler present in the cement. In fact, the C/S ratios measured are between 2 and 3, while in a common OPC they range from 1.5 to 2. Therefore, the calcium content of the calculated C/S ratios is overestimated due to the size of the microanalysis area and the presence of limestone filler microparticles within the cementitious matrix. Certain levels of Al and S (<5%) can always be seen with local EDS analyses. The oxide compositions and relative contents of Al and S in ettringite are the same in the initial ettringite and the newly formed one (EDS of Fig. 8 down-right). Thus, the ettringite-like phase has the same or a very similar chemical composition in both cases.

The EDS analyses carried out on the different phase appearances (dark-grey and light-grey) are shown in different compositions. The different local EDS analyses in dark and light grey zones are shown in Fig. 9 and compared with the results determined in the concrete of the Middle core. In this figure, the SiO<sub>2</sub>, CaO, Al<sub>2</sub>O<sub>3</sub> and SO<sub>3</sub> contents are shown on different graphs. The dark-grey zone shows a higher variability in the EDS analyses than the light-grey zone, but

general conclusions can be drawn. Both zones (dark-grey and light-grey) show slight decalcification with respect to the C-S-H gels of the concrete from the Middle core. The dark-grey zone shows a more similar composition to the C-S-H gels of the Middle core than the light-grey zone. However the light-grey zones have higher sulphate and alumina contents and remarkably lower silica contents. In fact, the composition of the light-grey zone is similar to that of ettringite (see Fig. 8). These results suggest a progressive alteration mechanism of C-S-H. First of all, the dissolution of portlandite and the decalcification of C-S-H could take place due to the interaction with the granite groundwater in the Up and Down zones. Then, the subsequent diffusion of sulphates from bentonite promotes that they interact with the C-S-H gels giving rise to their incorporation in the cement paste matrix. Thus, two different phases are formed: C-S-H with some decrease in calcium, incorporating Al and SO<sub>3</sub>, and another phase that progressively constitutes the secondary ettringite, according to some of the processes described by Menéndez et al. (2013).

Finally, the diffusion of Mg from the bentonite into the concrete close to the bentonite interface (<1 cm) is also detected although the measured Mg contents in the C-S-H gels are not very high (below 2% in most of the cases as shown in Fig. 10). In fact, as more

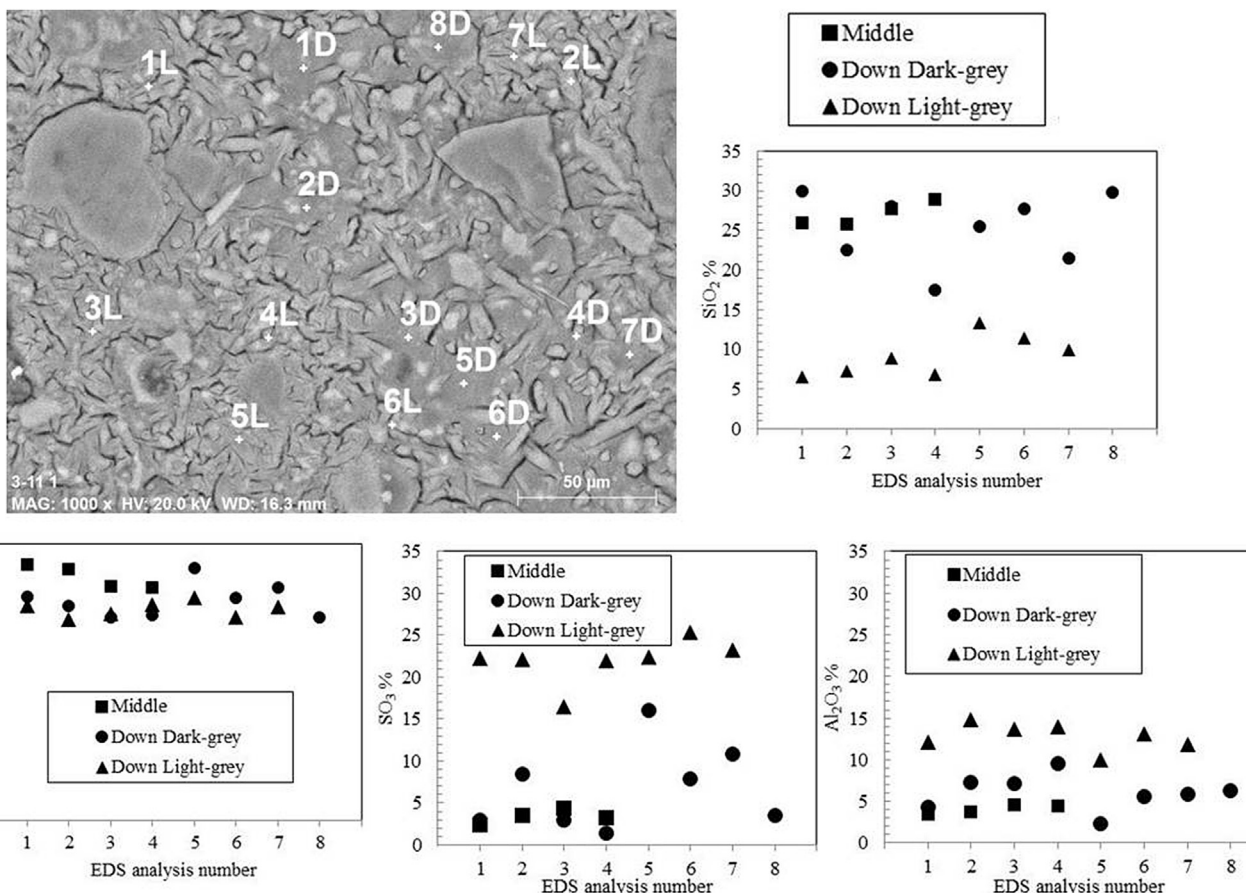


**Fig. 9.** % of oxide distribution in cement paste near the bentonite barrier or the dummy canister (<1 cm) for Middle core, Down core dark-grey zones and Down core light-grey zones. 1D: EDS analysis number 1 in dark zone; 1 L: EDS analysis number 1 in light zone. EDS numbers of Middle core refer to Fig. 8 BSEM image. Up-left: BSEM image of down core (x1000).

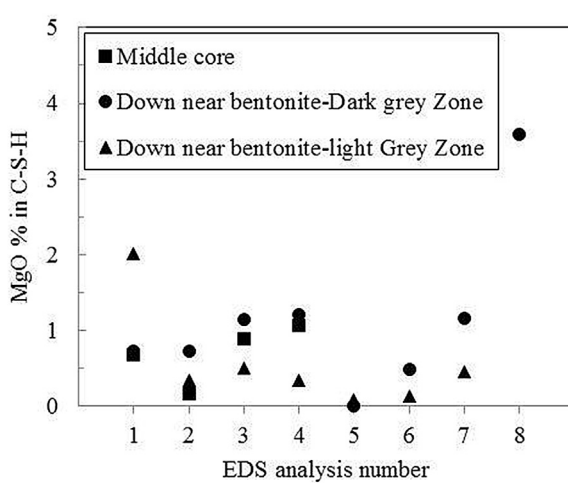


**Fig. 10.** MgO variation in C-S-H gels. The numbers of the EDS microanalysis are related with the BSEM images of Fig. 8 (for Middle core) and Fig. 9 (for Down core).

soluble Mg was found in the concrete pore solution, the possible future formation of M-S-H phases cannot be discarded, although this type of phenomena has been mainly detected in low-pH cementitious materials (García Calvo et al., 2010, 2013; Dauzères et al., 2016). In fact, in this case Mg concentrates in the bentonite part of the interface, with the concrete as an alkaline barrier for Mg

solubilisation and migration (Fernández et al., 2017).

#### 4. Conclusions

The FEBEX shotcreted concrete plug was dismantled after 13 years of operation. During this time concrete was in contact with the bentonite barrier and it was also interacting with the surrounding granite groundwater of the GTS. The influence of these interactions can be summarized as follows:

- The interaction of the granite groundwater with the concrete caused leaching processes in the concrete matrix with subsequent dissolution of portlandite. Pore solution pH values near or even below 12.5 were measured in the affected concrete. However, significant damage to the cementitious matrix from this groundwater-concrete interaction was not detected.
- The continuous action of the bentonite porewater caused many changes to the concrete matrix which was located at a depth lower than 5 cm from the bentonite-concrete interface. In fact, the first cm of the concrete plug in contact with the bentonite is the most altered zone. In this first centimetre the complete disappearance of portlandite could be seen, along with a massive ettringite formation. This secondary ettringite formation was due to the incorporation of sulphate which diffused from the bentonite barrier into the concrete matrix. The incorporation of Al and Mg in the C-S-H gels was seen. The progressive alteration of the initially formed C-S-H gels could be

noted at the bentonite-concrete interface. Finally, the diffusion of Cl ions from the bentonite barrier up to 5 cm into the concrete was detected and even the formation of small platelets of Friedel's salt could be distinguished within the cement paste.

## Acknowledgements

This work has been financially supported by the Full-Scale Engineered Barrier Experiment – Dismantling Project (FEBEX-DP) consortium (<http://www.grimsel.com/gts-phase-vi/FEBEX-dp>). Authors would like to acknowledge V. Flor-Laguna for her help in the experimental work.

## References

Adenot, F., Buil, M., 1992. Modelling of the corrosion of the cement paste by deionized water. *Cem. Concr. Res.* 22, 489–496.

Alonso, M.C., García Calvo, J.L., Pettersson, S., Puigdomenech, I., Cuñado, M., Vuorio, A.M., Weber, H., Ueda, H., Naito, M., Walker, C., Takeshi, Y., Cau-dit-Coumes, C., 2013. Round robin test for defining an accurate protocol to measure the pore fluid pH of low-pH cementitious materials. In: Bart, F., Cau-dit-Coumes, C., Frizon, F., Lorente, S. (Eds.), *Cement-based Materials for Nuclear Waste Storage*. Springer, pp. 251–259.

Bárcena, I., García-Síneriz, J.L., 2015. FEBEX-DP (GTS) Full Dismantling Sampling Plan. Nagra Report NAB, p. 15, 14.

Buil, B., Gómez, P., Peña, J., Garralón, A., Turrero, M.J., Escribano, A., Sánchez, L., Durán, J.M., 2010. Modelling of bentonite–granite solutes transfer from an in situ full-scale experiment to simulate a deep geological repository (Grimsel Test Site, Switzerland). *Appl. Geochem.* 25, 1797–1804.

Carde, C., François, R., 1999. Modelling the loss of strength and porosity increase due to the leaching of cement pastes. *Cem. Concr. Compos.* 21, 181–188.

Cuevas, J., Ruiz, A.I., Fernández, R., Torres, E., Escribano, A., Regadío, M., Turrero, M.J., 2016. Lime mortar-compacted bentonite–magnetite interfaces: an experimental study focused on the understanding of the EBS long-term performance for high-level nuclear waste isolation DGR concept. *Appl. Clay Sci.* 124–125, 79–93.

Dauzères, A., Le Bescop, P., Sardini, P., Cau Dit Coumes, C., 2010. Physico-chemical investigation of clayey/cement-based materials interaction in the context of geological waste disposal: experimental approach and results. *Cem. Concr. Res.* 40, 1327–1340.

Dauzères, A., Achiedo, G., Nied, D., Bernard, E., Alahache, S., Lothenbach, B., 2016. Magnesium perturbation in low-pH concretes placed in clayey environmental-solid characterizations and modelling. *Cem. Concr. Res.* 79, 137–150.

Dehwah, H.A.F., 2007. Effect of sulphate concentration and associated cation type on concrete deterioration and morphological changes in cement hydrates. *Constr. Build. Mater.* 21, 29–39.

ENRESA, 2006. FEBEX Project Final Report. Post-mortem Bentonite Analysis, Enresa Publicación Técnica 05–1/2006.

Faucon, P., Adenot, F., Jordá, M., Cabrilac, R., 1997. Behaviour of crystallised phases of Portland cement upon water attack. *Mater. Struct.* 30, 480–485.

Faucon, P., Adenot, F., Jaquinot, J.F., Petit, C., Cabrilac, R., Jordá, M., 1998. Longterm behaviour of cement pastes used for nuclear waste disposal: review of physico-chemical mechanisms of water degradation. *Cem. Concr. Res.* 28, 847–857.

Fernández, A.M., Baeyens, B., Bradbury, M., Rivas, P., 2004. Analysis of the porewater chemical composition of a Spanish compacted bentonite used in an engineered barrier. *Parts A/B/C* 29 *Phys. Chem. Earth* 105–118.

Fernández, R., Mäder, U., Rodríguez, M., Virgil de la Villa, R., Cuevas, J., 2009. Alteration of compacted bentonite by diffusion of highly alkaline solutions. *Eur. J. Mineral.* 21, 725–735.

Fernández, A.M., Villar, M.V., 2010. Geochemical behaviour of a bentonite barrier in the laboratory after up to 8 years of heating and hydration. *Appl. Geochem.* 25, 809–924.

Fernández, R., Torres, E., Ruiz, A.I., Cuevas, J., Alonso, M.C., García Calvo, J.L., Rodríguez, E., Turrero, M.J., 2017. Interaction processes at the concrete-bentonite interface after 13 years of FEBEX-Plug operation. Part II: bentonite contact. *Parts A/B/C* (in this issue). *Phys. Chem. Earth*.

García Calvo, J.L., Hidalgo, A., Alonso, C., Fernández Luco, L., 2010. Development of low-pH cementitious materials for HLRW repositories. Resistance against ground waters aggression. *Cem. Concr. Res.* 40, 1290–1297.

García Calvo, J.L., Alonso, M.C., Hidalgo, A., Fernández Luco, L., Flor-Laguna, V., 2013. Development of low-pH cementitious materials based on CAC for HLW repositories: long-term hydration and resistance against groundwater aggression. *Cem. Concr. Res.* 51, 67–77.

García-Síneriz, J.L., Abós, H., Martínez, V., De la Rosa, C., Mäder, U., Kober, F., 2016. FEBEX DP: Dismantling of Heater 2 at the FEBEX “in Situ” Test. Description of Operations. Nagra Report NAB 16–11.

Garralón, A., Gómez, P., Peña, J., Sánchez, L., Buil, B., Turrero, M.J., Torres, E., 2016. Hydrogeochemical Characterization of the FEBEX Gallery. Report CIEMAT/DMA/2G216/7/16.

Gaucher, E.C., Blanc, P., 2006. Cement/clay interactions – a review: experiments, natural analogues, and modeling. *Waste Manag.* 26, 776–788.

Huertas, F., Fariñas, P., Farias, J., García-Síneriz, J.L., Villar, M.V., Fernández, A.M., Martín, P.L., Elorza, F.J., Gens, A., Sánchez, M., Lloret, A., Samper, J., Martínez, M.A., 2006. Full-scale Engineered Barriers Experiment. Updated Final Report 1994–2004. Enresa, Technical Report 05–0/2006.

Irassar, E.F., Bonavetti, V.L., González, M., 2003. Microstructural study of sulphate attack on ordinary and limestone Portland cements at ambient temperature. *Cem. Concr. Res.* 33, 31–41.

Jenni, A., Mäder, U., Lerouge, C., Gaboreau, S., Schwyn, B., 2014. In situ interaction between different concretes and opalinus clay. *Parts A/B/C* 70–71 *Phys. Chem. Earth* 71–83.

Kamali, S., Gérard, B., Moranville, M., 2003. Modelling the leaching kinetics of cement based materials – influence of materials and environment. *Cem. Concr. Compos.* 25, 451–454.

Kari, O.P., Puttonen, J., 2014. Simulation of concrete deterioration in Finnish rock cavern conditions for final disposal of nuclear waste. *Ann. Nucl. Energy* 72, 20–30.

Lagerblad, B., 1999. In: *Texture and Chemistry of Historic Concrete Subjected to Prolonged Hydration. Workshop on Water in Cement Paste and Concrete Hydration and Pore Structure*. Nordic Concr. Fed., Skagen, pp. 148–154.

Lipus, K., Punkte, S., 2003. Sulfatwiderstand unterschiedlich zusammengesetzter betone. *TI.1 — Sulphate Resist. Concr. Differ. Compos. (Part 1)*, Beton — Duseldorff 53, 97–101.

Lovera, P., le Bescop, P., Adenot, F., Li, G., Tanaka, Y., Owaki, E., 1997. Physicochemical transformations of sulphated compounds during the leaching of highly sulphated cement wastes. *Cem. Concr. Res.* 27, 1523–1532.

Mainguy, M., Tognazzi, C., Torrenti, J.-M., Adenot, F., 2000. Modelling of leaching in pure cement paste and mortar. *Cem. Concr. Res.* 30, 83–90.

Maltais, Y., Samson, E., Marchand, J., 2004. Predicting the durability of Portland cement systems in aggressive environments — laboratory validation. *Cem. Concr. Res.* 34, 1579–1589.

Martínez, V., Abós, H., García-Síneriz, J.L., 2016. Final Sensor Data Report (FEBEX “in Situ” Experiment). Nagra Report NAB 16–19.

Menéndez, E., Matschei, T., Glasser, F.P., 2013. Sulphate attack of concrete. In: Mark, A., Bertron, A., De Belie, N. (Eds.), *Performance of Cement-based Materials in Aggressive Aqueous Environments State-of-The-Art Report*, RILEM TC 211 – PAE Series: RILEM State-of-the-art Reports, vol. 10. Springer 462, pp. 7–71. XVI.

Moranville, M., Kamali, S., Guillou, E., 2004. Physicochemical equilibria of cement-based materials in aggressive environments — experiment and modeling. *Cem. Concr. Res.* 34, 1569–1578.

Neville, A., 2004. The confused world of sulphate attack on concrete, review. *Cem. Concr. Res.* 34, 1275–1296.

Sánchez, L., Cuevas, J., Ramírez, S., Riuizdeleon, D., Fernandez, R., Vigildelavilla, R., Leguay, S., 2006. Reaction kinetics of FEBEX bentonite in hyperalkaline conditions resembling the cement–bentonite interface. *Appl. Clay Sci.* 33, 125–141.

Santhanam, M., 2013. *Performance of Cement-based Materials in Aggressive Aqueous Environments. Part I. Mechanisms of Degradation of Cementitious Materials in Aggressive Aqueous Environments. Magnesium Attack of Cementitious Materials in Marine Environments*. Springer Verlag.

Soler, J.M., Mäder, U.K., 2007. Mineralogical alteration and associated permeability changes induced by a high-pH plume: modeling of a granite core infiltration experiment. *Appl. Geochem.* 22, 17–29.

Tixier, R., Mobasher, B., 2003. Modeling of damage in cement-based materials subjected to external sulphate attack. I: formulation. *J. Mater. Civ. Eng.* 15 (4), 305–313.

Wang, J., 2014. On area-specific underground research laboratory for geological disposal of high-level radioactive waste in China. *J. Rock Mech. Geotech. Eng.* 6, 99–104.

Yamamoto, T., Imoto, H., Ueda, H., Hironaga, M., 2007. Leaching alteration of cementitious materials and release of organic additives – study by Numo and Cipriani, R&D on low-pH cement for a geological repository. 3rd Workshop Paris June, pp. 52–61.